Pergamon

Int. J. Solids Structures Vol. 35, Nos 9–10, pp. 831–854, 1998

0020–7683/98 $19.00 + .00

PII: S0020–7683(97)00083–8

THE DYNAMICAL ANALYSIS OF A FINITE INEXTENSIBLE BEAM WITH AN ATTACHED ACCELERATING MASS

YI-MING WANG

Division of Automobile Technology, Department of Industrial Education, College of Technology, National Chunghua Normal University, Shih-ta Road, Chunghua, Taiwan, Republic of China

(*Received* 3 *August* 1996; *in revised form* 5 *March* 1997)

Abstract—The objective of this paper is an analytical and numerical study of the dynamics of a beam with attached masses. Specifically, a finite inextensible beam that rests on a uniform elastic foundation and carries an accelerating mass is considered. Of interest is the dynamics of the beam-mass system due to the motion of the moving mass. The influence of various parameters such as forward force, retard force and friction upon the performance of the beam are investigated. The mechanics of the problem is Newtonian. Based on the assumption that when the moving mass is set in motion the mass is assumed to be rolling on the beam, the mechanics, including effects due to friction and convective accelerations of the interface between the moving mass and the beam, are determined. The problem of the system is nonlinear, due to the presence of friction and the convective acceleration. In the modeling, the mass can be accelerated by a force. Meanwhile, the mass is capable of reducing speed and being brought to a stop at any position on the beam by applying a retard force to the mass and/or increasing the friction between the mass and the beam. The force is assumed to be tangential to the deformed configuration of the beam. By employing the Galerkin procedure, the partial differential equations which describe the transient vibrations of the beam-mass system are reduced to an initial value problem with finite dimensions. The method of numerical integration is used to get convergent solutions. © 1997 Elsevier Science Ltd.

INTRODUCTION

Vibrations of flexible structures with attached moving masses have been the subject of many studies. A basic understanding of the underlying phenomena is vital to control these vibrations and save operations of the system. Florence (1965) considered the velocity distribution of a semi-infinite Timoshenko beam under a constant force that travels with a constant velocity. His results show that, in the case when the load speed is equal to the shear wave velocity, there is a discontinuity at the shear wavefront, which increases indefinitely with the load along the beam exists.

Steele (1967) investigated the response of a simple supported finite beam with and without an elastic foundation under a moving load. He points out that the vibrations decrease exponentially with the distance from the load when the load speed is low and does not exceed a critical speed. In a later study, Steele (1968) analyzed the response of a semi-infinite Timoshenko beam on an elastic foundation under a step load that moves with constant velocity along the beam. He shows the impossibility of the occurrence of a steady-state when the load speed is equal to either the shear or the bar velocity. He verifies that the transients due to the end condition never die out but continue to remain in the vicinity of the load front. He also indicates that the non-existence of a steady-state does not imply the existence of a critical condition, therefore, only one truly critical speed exists.

The problem of oscillations of beams with attached moving masses, in which the inertia term of the riding particles is taken into account, has been considered by many authors. Nelson and Conover (1971) investigated the dynamic stability of a simple supported Bernoulli–Euler beam on an elastic foundation under a series of equally spaced masses that move with a constant speed. The regions of dynamic instability of response are determined by the Floquet theory. Their results indicate that the stiffness of the beam and the elastic foundation increase with the number of attached masses.

Ayre *et al.* (1951) analyzed the response of one- and two-span beam carrying a moving mass load. Three different conditions are considered in their analysis. The two former problems are related to a beam with negligible mass and a load with negligible mass, respectively. The general case, in which the masses of the beam and moving load are encountered, are considered in the third case. The results of their study show that the inertia term of moving mass amplifies the higher modes of vibrations of the system.

Ting *et al.* (1974) considered the interaction between the moving mass and the supporting structure. They pointed out that the convective acceleration terms not previously recognized should be included if a "correct" formulation is desired. In a later study, Alexsandradis *et al.* (1978) modeled the dynamic interaction problem between a spring-mass-damper element and its supporting rail as a prestressed continuously supported, infinitely long beam. Their results indicate that the system is dynamically unstable if a certain value of critical velocity is exceeded.

Tadjbakhsh and Wang (1993) and Wang (1993) analyzed the transient vibrations of a taut inclined cable with a riding accelerating mass. They developed a new model that includes the effect of rolling friction between the rollers of the trolley, the moving mass and the cable. An important feature to be carried out in their analysis is the ability to bring the trolley to a halt at the end point of the cable. This is achieved by applying a reverse thrust to the trolley. This approach is also the basis of this study to investigate the dynamics of a beam-mass system due to the motion of the attached mass. In this study, the transient vibrations of a finite inextensible beam, with a riding accelerating mass, are investigated. The beam rests on a uniform elastic foundation. The gravity of the beam then is assumed to be taken by the foundation preload.

When the moving mass is set in motion, the mechanics, involving effects due to friction and convective accelerations, of the interface between the moving mass and the beam are determined. The mass can be accelerated by a forward force. Meanwhile, the mass may reduce speed and brake to a halt at a desired position on the beam by applying a reverse force to the mass and/or increasing the friction between the mass and the beam. Unlike other papers, in which either the velocity or the acceleration of moving mass is held to be constant, in this study the propelling and retarding forces on the moving mass are specified. This results in variable velocity and acceleration, and unknown location of the mass along the beam.

BASIC FORMULAS

In this study, a finite inextensible beam rested on a uniform elastic foundation and having a length of l is considered. The static state of the beam is obtained by assuming that the gravity of the beam and the foundation preload are in the state of equilibrium. The Cartesian position vector of point s along the beam at time t is represented by $\mathbf{r}(s, t)$ and is given as (Fig. 1)

$$\mathbf{r}(s, t) = (x(s) + u(s, t))\mathbf{i} + v(s, t)\mathbf{j} \tag{1}$$

where $u(s, t)$ and $v(s, t)$ are the axial displacement and the transverse displacement of the beam from the undeformed state, respectively.

The equations governing the motion of the system can be derived from the dynamic equilibrium of forces and momenta. From Figs. 1 and 2, one obtains

$$\mathbf{F}_{,s} + \mathbf{f} = m\mathbf{r}_{,tt}, \quad 0 < s < l, \quad t > 0 \tag{2}$$

$$-\bar{M}_{,s} + V = 0 \tag{3a}$$

$$\bar{M} = -EIv_{,ss} \tag{3b}$$

with the inextensibility constraint

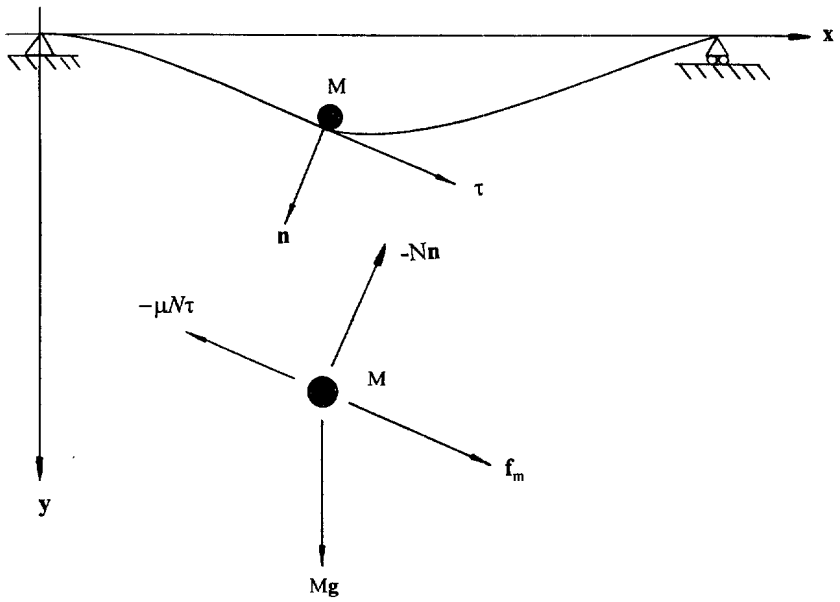

Fig. 1. System configuration.

$$\mathbf{r}_{,s} \cdot \mathbf{r}_{,s} = 1, \tag{4}$$

where the subscript s and t denote the s and t differentiation and where m indicates the mass per unit length of the beam. E and I are the Young's modulus and the area moment of inertia of the beam. $\mathbf{f}$ denotes the mass per unit length of the beam and the external forces including the weight of the moving mass and the moving reaction of the mass upon the beam and

$$\mathbf{F} = H\mathbf{i} + P\mathbf{j} = T\boldsymbol{\tau} + V\mathbf{n} = (T\cos\theta - V\sin\theta)\mathbf{i} + (T\sin\theta + V\cos\theta)\mathbf{j} \tag{5}$$

where T is the axial force in the beam; V is the transverse force in the beam; and θ is the angle between the neutral axis of the beam and the x-axis.

The equation of motion of the moving mass obeys (Fig. 1)

$$M\mathbf{a}_M = M\boldsymbol{g} + \mathbf{f}_m - \mu N\boldsymbol{\tau} - N\mathbf{n}, \tag{6}$$

where M, N and μ denote the mass of the moving mass, the reaction of beam on the mass, and the coefficient of friction, respectively, and $\boldsymbol{g} = g\mathbf{j}$ = acceleration of gravity, $\mathbf{f}_m$ = force acting on the mass, $\boldsymbol{\tau}$ = unit tangent vector to the beam configuration = $(1-u_{,s})\mathbf{i} + v_{,s}\mathbf{j} = \cos\theta\mathbf{i} + \sin\theta\mathbf{j}$, $\mathbf{n}$ = unit normal vector to the beam configuration = $v_{,s}\mathbf{i} + (1+u_{,s})\mathbf{j} = -\sin\theta\mathbf{i} + \cos\theta\mathbf{j}$.

The acceleration of the moving mass, $\mathbf{a}_M$, is obtained from

$$\mathbf{a}_M = \frac{d^2}{dt^2}[\mathbf{r}(\bar{s}(t), t)] = \mathbf{r}_{,ss}(\bar{s}_{,t})^2 + 2\mathbf{r}_{,st}\bar{s}_{,t} + \mathbf{r}_{,s}\bar{s}_{,tt} + \mathbf{r}_{,tt} \tag{7}$$

in which $\bar{s}(t)$ is the distance along the arc of the beam which represents the position of the moving mass. The force $\mathbf{f}$ on the beam can be stated by

$$\mathbf{f} = -kv\mathbf{j} + (N\mathbf{n} + \mu N\boldsymbol{\tau})\delta(s-\bar{s}), \tag{8}$$

where k is the foundation stiffness per unit length and $\delta(s-\bar{s})$ is the Dirac delta function.

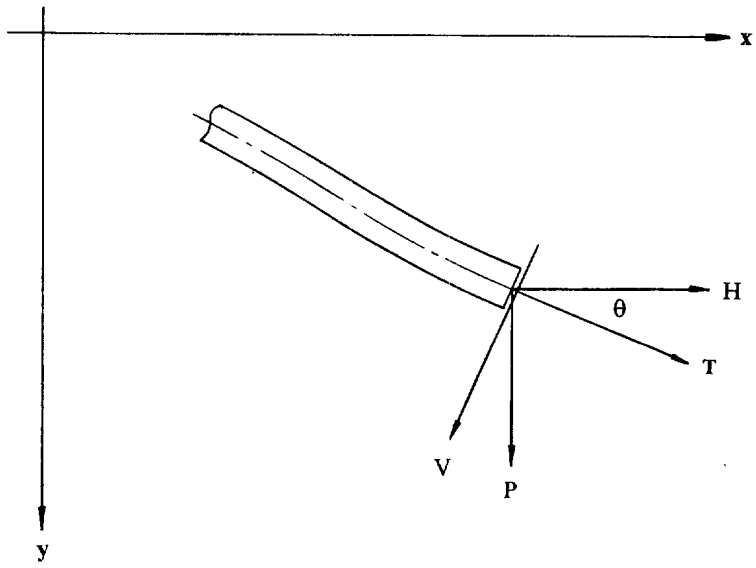

Fig. 2. Force equilibrium diagram.

As mentioned previously, whenever a mass is being propelled by a force along a beam the force on the mass will be along the tangent to the vibrating beam. Hence, the force acting on the moving mass has the form

$$\mathbf{f}_m = Mf\boldsymbol{\tau} = Mf[(1+u_{,s})\mathbf{i}+v_{,s}\mathbf{j}], \tag{9}$$

where f is a prescribed function of time. For example, f may be a positive constant to increase speed and a negative constant to reduce speed and to come to a stop at a desired position on the beam.

By substitution of eqns (1) and (5) with eqn (3) into eqn (2), the equations of motion of the combined system in directions **i** and **j** yield

$$[T(1+u_{,s})+EIv_{,sss}v_{,s}]_{,s}+\mathbf{f}_m\cdot\mathbf{i}\delta(s-\bar{s}) = mu_{,tt}+M[u_{,ss}(\bar{s}_{,t})^2+2u_{,st}\bar{s}_{,t}+(1+u_{,s})\bar{s}_{,tt}+u_{,tt}]\delta(s-\bar{s}),$$
$$0<s<l, \quad t>0 \tag{10}$$

$$[Tv_{,s}-EIv_{,sss}(1+u_{,s})]_{,s}+(\mathbf{f}_m\cdot\mathbf{j}+Mg)\delta(s-\bar{s})$$
$$= mv_{,tt}+kv+M[v_{,ss}(\bar{s}_{,t})^2+2v_{,st}\bar{s}_{,t}+v_{,s}\bar{s}_{,tt}+v_{,tt}]\delta(s-\bar{s}),0<s<l, \quad t>0. \tag{11}$$

Similarly, considering the equation of motion of the moving mass, eqn (6), one has

$$M[u_{,ss}(\bar{s}_{,t})^2+2u_{,st}\bar{s}_{,t}+(1+u_{,s})\bar{s}_{,tt}+u_{,tt}] = \mathbf{f}_m\cdot\mathbf{i}+N[v_{,s}-\mu(1+u_{,s})], s=\bar{s}(t), \quad t>0 \tag{12}$$

$$M[v_{,ss}(\bar{s}_{,t})^2+2v_{,st}\bar{s}_{,t}+v_{,s}\bar{s}_{,tt}+v_{,tt}] = (\mathbf{f}_m\cdot\mathbf{j}+Mg)-N[\mu v_{,s}+(1+u_{,s})], s=\bar{s}(t), \quad t>0. \tag{13}$$

Eliminating N between the above two equations and using eqn (4), the result yields

$$(1+u_{,s}^2)\bar{s}_{,tt}-[\mu v_{,ss}-v_{,s}v_{,ss}-u_{,ss}+\mu(u_{,s}v_{,ss}-u_{,ss}v_{,s})](\bar{s}_{,t})^2$$
$$-2[\mu v_{,st}-v_{,st}v_{,s}-u_{,st}+\mu(u_{,s}v_{,st}-u_{,st}v_{,s})]\bar{s}_{,t}$$
$$= g[v_{,s}-\mu(1+u_{,s})]+f\{(1+u_{,s})[\mu v_{,s}+(1+u_{,s})]+v_{,s}[v_{,s}-\mu(1+u_{,s})]\}$$
$$-v_{,tt}[v_{,s}-\mu(1+u_{,s})]-u_{,tt}[\mu v_{,s}+(1+u_{,s})], \quad s=\bar{s}(t), \quad t>0. \tag{14}$$

Equations (4), (10), (11) and (14) accounts for $u(s,t)$, $v(s,t)$, T and $\bar{s}$ when m, M, μ, g and the boundary conditions are specified.

In this study, the system under consideration is a finite, simply-supported, Bernoulli–Euler beam on a uniform elastic foundation with a riding accelerating mass. Hence, the longitudinal displacement of the beam vanishes at $s = 0$; the resultant in the i-direction vanishes at $s = l$. The moment and transverse displacement also vanish at $s = 0, l$. Then, the boundary conditions are:

$$u(0,t) = v(0,t) = v(l,t) = \frac{\partial^2 v(0,t)}{\partial s^2} = \frac{\partial^2 v(l,t)}{\partial s^2} = 0 \tag{15}$$

$$H(l,t) = T(l,t)(1+u_{,s}) + EIv_{,sss}v_{,s} = 0, \quad \text{at } s = l. \tag{16}$$

To determine the axial force T, we return to eqn (10). Based on the assumption that the variation of axial force is assumed to remain continuous at $s = \bar{s}(t)$, we integrate eqn (10) and use the boundary condition, eqn (16). After some manipulations, the result yields

$$T(s,t) = \frac{-1}{1+u_{,s}}[EIv_{,sss}v_{,s} + \int_s^l mu_{,tt}\,\mathrm{d}s], \quad 0 < s < l, \quad t > 0. \tag{17}$$

It is mentioned here that from eqn (4) we found that the axial displacement $u(s,t)$ is in the second-order of nonlinearity of the transverse displacement $v(s,t)$. Hence, the axial force of the beam $T(s,t)$ in eqn (17) is also in the second-order of nonlinearity of $v(s,t)$.

The equations of motion of the beam–mass system, eqns (11) and (14) with eqn (17), in dimensionless form can be obtained by introducing the following dimensionless quantities:

$$\tau = \sqrt{\frac{EI}{ml^4}}\,t, \quad \hat{M} = \frac{M}{ml}, \quad \hat{T} = \frac{ml^2}{EI}T, \quad \hat{f} = \frac{ml^4}{EI}f,$$
$$\hat{g} = \frac{ml^4}{EI}g, \quad \hat{k} = \frac{kl^4}{EI}, \quad \eta = \frac{s}{l}, \quad \xi = \frac{\bar{s}}{l}, \quad \hat{v} = \frac{v}{l}, \quad \hat{u} = \frac{u}{l} \tag{18}$$

then eqns (17), (11) and (14) become, respectively,

$$\hat{T}(\eta,\tau) = \frac{-1}{1+\hat{u}'}\left[\hat{v}'''\hat{v}' + \int_\eta^1 \ddot{\hat{u}}\,\mathrm{d}\eta\right], \quad 0 < \eta < 1, \quad \tau > 0, \tag{19}$$

$$[\hat{T}\hat{v}' - \hat{v}'''(1+\hat{u}')]' + \hat{M}(\hat{f}\hat{v}' + \hat{g})\delta(\eta-\xi)$$
$$= \ddot{\hat{v}} + \hat{k}\hat{v} + \hat{M}[\hat{v}''(\dot{\xi})^2 + 2\ddot{\hat{v}}'\dot{\xi} + \hat{v}'\ddot{\xi} + \ddot{\hat{v}}]\delta(\eta-\xi), \quad 0 < \eta < 1, \quad \tau > 0, \tag{20}$$

$$(1+\hat{u}'^2)\ddot{\xi} - [\mu\ddot{\hat{v}}'' - \ddot{\hat{v}}'\hat{v}'' - \ddot{\hat{u}}'' + \mu(\hat{u}'\hat{v}'' - \hat{u}''\hat{v}')](\dot{\xi})^2$$
$$-2[\mu\ddot{\hat{v}}' - \ddot{\hat{v}}'\hat{v}' - \ddot{\hat{u}}' + \mu(\hat{u}'\ddot{\hat{v}}' - \ddot{\hat{u}}'\hat{v}')]\dot{\xi}$$
$$= \hat{g}[\hat{v}' - \mu(1+\hat{u}')] + \hat{f}\{(1+\hat{u}')[\mu\hat{v}' + (1+\hat{u}')] + \hat{v}'[\hat{v}' - \mu(1+\hat{u}')]\}$$
$$-\ddot{\hat{v}}[\hat{v}' - \mu(1+\hat{u}')] - \ddot{\hat{u}}[\mu\hat{v}' + (1+\hat{u}')], \quad \eta = \xi, \quad \tau > 0, \tag{21}$$

where a superposed prime and a dot denote the η and τ differentiation.

Here, we consider small deformations. For this, we neglect nonlinear timers when we compare these terms to the linear time of $v(s,t)$ and unity. The equation of motion of the beam, eqn (20), then can be simplified as

$$\ddot{\hat{v}}+\hat{v}''''+\hat{k}\hat{v}+\hat{M}[\hat{v}''(\dot{\xi})^2+2\dot{\hat{v}}'\dot{\xi}+\hat{v}'\ddot{\xi}+\ddot{\hat{v}}-\hat{f}\hat{v}']\delta(\eta-\xi)=\hat{M}\hat{g}\delta(\eta-\xi),$$
$$0<\eta<1,\quad \tau>0, \tag{22}$$

while the equation of motion of the moving mass, eqn (21), becomes

$$\ddot{\xi}-\mu\hat{v}''(\dot{\xi})^2-2\mu\dot{\hat{v}}'\dot{\xi}=\hat{f}-\mu\hat{g}+\hat{g}\hat{v}'+\mu\dot{\hat{v}},\quad \eta=\xi,\quad \tau>0. \tag{23}$$

Examination of the dynamics governed by eqns (22) and (23) is the main purpose in this study. As shown in eqn (23), the problem is nonlinear due to the existence of convective acceleration and friction between the moving mass and the beam.

We being by representing $\hat{v}$ as a continuous function. Let

$$\hat{v}=\sum_{n=1}^{\infty}A_n(\tau)\sin n\pi\eta,\quad 0<\eta<1,\quad \tau>0. \tag{24}$$

Thus, the boundary condition, eqn (15), is satisfied. Next, eqn (24) is substituted into eqns (22) and (23), respectively, which yields

$$\sum_{n=1}^{\infty}\{[\ddot{A}_n(\tau)+((n\pi)^4+\hat{k})A_n(\tau)]\sin n\pi\eta\}+\hat{M}\sum_{n=1}^{\infty}\{[\ddot{A}_n(\tau)-(n\pi)^2\dot{\xi}^2A_n(\tau)]\sin n\pi\eta$$
$$+(n\pi)[2\dot{\xi}\dot{A}_n(\tau)+\ddot{\xi}A_n(\tau)-\hat{f}A_n(\tau)]\cos n\pi\eta\}\delta(\eta-\xi)=\hat{M}\hat{g}\delta(\eta-\xi),\quad 0<\eta<1,\quad \tau>0 \tag{25}$$

$$\ddot{\xi}+\mu\left(\sum_{n=1}^{\infty}(n\pi)^2A_n(\tau)\sin n\pi\xi\right)\dot{\xi}^2-2\mu\left(\sum_{n=1}^{\infty}(n\pi)\dot{A}_n(\tau)\cos n\pi\xi\right)\dot{\xi}$$
$$=(\hat{f}-\mu\hat{g})+\hat{g}\sum_{n=1}^{\infty}(n\pi)A_n(\tau)\cos n\pi\xi+\mu\sum_{n=1}^{\infty}\dot{A}_n(\tau)\sin n\pi\xi,\quad \tau>0. \tag{26}$$

The approximate solution of the beam–mass system can be obtained by employing Galerkin's method. Using Galerkin's procedure for minimizing error, we multiply eqn (25) by $\sin j\pi\eta$ and integrate eqn (25) with respect to η from zero to 1, thus obtaining

$$\ddot{A}_j(\tau)+2\hat{M}\sum_{n=1}^{\infty}\hat{S}_{jn}(\xi)\ddot{A}_n(\tau)+4\hat{M}\dot{\xi}\sum_{n=1}^{\infty}R_{jn}(\xi)\dot{A}_n(\tau)+[(j\pi)^4+\hat{k}]A_j(\tau)$$
$$+2\hat{M}\sum_{n=1}^{\infty}[(\ddot{\xi}-\hat{f})R_{jn}(\xi)-(\dot{\xi})^2S_{jn}(\xi)]A_n(\tau)=2\hat{M}\hat{g}\hat{S}_j(\xi),0<\eta<1,\quad \tau>0. \tag{27}$$

Also the equation of motion of the moving mass, eqn (26), becomes

$$\ddot{\xi}+\mu\sum_{n=1}^{\infty}S_n(\xi)A_n(\tau)(\dot{\xi})^2-2\mu\sum_{n=1}^{\infty}C_n(\xi)\dot{A}_n(\tau)\dot{\xi}$$
$$=(\hat{f}-\mu\hat{g})+\hat{g}\sum_{n=1}^{\infty}C_n(\xi)A_n(\tau)+\mu\sum_{n=1}^{\infty}\hat{S}_n(\xi)\ddot{A}_n(\tau),\quad \tau>0 \tag{28}$$

where

$$\hat{S}_{jn}(\xi)=\sin n\pi\xi\sin j\pi\xi,\quad S_{jn}(\xi)=(n\pi)^2\sin n\pi\xi\sin j\pi\xi=(n\pi)^2\hat{S}_{jn}(\xi),$$
$$\hat{R}_{jn}(\xi)=\cos n\pi\xi\sin j\pi\xi,\quad R_{jn}(\xi)=(n\pi)\cos n\pi\xi\sin j\pi\xi=(n\pi)\hat{R}_{jn}(\xi),$$
$$\hat{S}_n(\xi)=\sin n\pi\xi,\quad S_n(\xi)=(n\pi)^2\sin n\pi\xi=(n\pi)^2\hat{S}_n(\xi),$$
$$\hat{C}_n(\xi)=\cos n\pi\xi,\quad C_n(\xi)=(n\pi)\cos n\pi\xi=(n\pi)\hat{C}_n(\xi).$$

To write the equations of motion in matrix form, we allow j and n in eqns (27) and (28) to have the range

$$j = 1, 2, 3, \ldots, N$$

$$n = 1, 2, 3, \ldots, N$$

and let

$$\mathbf{y} = (A_1, A_2, \ldots, A_N)^T. \tag{29}$$

Then eqns (27) and (28) can be written as

$$\mathbf{M}(\xi)\ddot{\mathbf{y}}(\tau) + \dot{\xi}\mathbf{N}(\xi)\dot{\mathbf{y}}(\tau) + \mathbf{K}_1(\xi)\mathbf{y} + \ddot{\xi}\mathbf{K}_2(\xi)\mathbf{y} + \dot{\xi}^2\mathbf{J}_3(\xi)\mathbf{y} = \mathbf{h}(\xi) \tag{30}$$

and

$$\ddot{\xi} + p(\xi, \mathbf{y})\dot{\xi}^2 + q(\xi, \dot{\mathbf{y}})\dot{\xi} + \tilde{\mathbf{s}}^T(\xi)\ddot{\mathbf{y}} + \tilde{\mathbf{c}}^T(\xi)\mathbf{y} = f^*, \tag{31}$$

respectively. The initial conditions are

$$\dot{\mathbf{y}}(0) = \mathbf{y}(0) = \mathbf{0} \quad \text{and} \quad \xi(0) = 0 \tag{32}$$

where the components of the previously defined matrices, vectors and scalars in eqns (30) and (31), i.e. $\mathbf{M}$, $\mathbf{N}$, $\mathbf{K}_1$, $\mathbf{K}_2$, $\mathbf{K}_3$, $\mathbf{h}$, p, q, $\tilde{\mathbf{c}}$, $\tilde{\mathbf{s}}$ and f^* are given in the Appendix.

In order to obtain the numerical integration scheme of the system with the associated initial conditions as specified in eqn (32), we introduce state vectors into the second-order differential equations, eqns (30) and (31). To do this, we let

$$\mathbf{z} = (\dot{\mathbf{y}}^T, \dot{\xi}, \mathbf{y}^T, \xi)^T \tag{33}$$

where $\mathbf{z}$ is the $2N+2$ vector with the initial condition $\mathbf{z}(0) = \mathbf{0}$. Then eqns (30) and (31) can be written as

$$\tilde{\mathbf{M}}\dot{\mathbf{z}} + \tilde{\mathbf{N}}\mathbf{z} + \tilde{\mathbf{f}} = \mathbf{0}. \tag{34}$$

In eqn (34), $\tilde{\mathbf{M}}$ and $\tilde{\mathbf{N}}$ are $(2N+2) \times (2N+2)$ matrices and $\tilde{\mathbf{f}}$ is the $2N+2$ vector defined by

$$\tilde{\mathbf{M}} = \begin{bmatrix} \mathbf{M} & \mathbf{K}_2\mathbf{y} & \dot{\xi}\mathbf{N} & \mathbf{0} \\ \tilde{\mathbf{s}}^T & 1 & \mathbf{0}^T & \dot{\xi}p \\ [\mathbf{0}] & \mathbf{0} & \mathbf{I} & \mathbf{0} \\ \mathbf{0}^T & 0 & \mathbf{0}^T & 1 \end{bmatrix}$$

$$\tilde{\mathbf{N}} = \begin{bmatrix} [\mathbf{0}] & \mathbf{0} & \mathbf{K}_1 + \dot{\xi}^2\mathbf{K}_3 & \mathbf{0} \\ \mathbf{0}^T & q & \tilde{\mathbf{c}}^T & 0 \\ -\mathbf{I} & \mathbf{0} & [\mathbf{0}] & \mathbf{0} \\ \mathbf{0}^T & -1 & \mathbf{0}^T & 0 \end{bmatrix}$$

$$\tilde{\mathbf{f}} = (-\mathbf{h}^T, -f^*, \mathbf{0}^T, 0)^T$$

where $\mathbf{I}$, $[\mathbf{0}]$ and $\mathbf{0}$ are the $N \times N$ unit, $N \times N$ zero and $N \times 1$ zero matrices, respectively.

NUMERICAL RESULTS AND DISCUSSIONS

Numerical results refer to an assumed model wherein a finite inextensible beam rests on a uniform elastic foundation and carries an accelerating mass rolling on it. The moving mass is to be accelerating by a positive driving force and can be brought to a halt at desired point on the beam by a simulated braking system. In the system, the applied reverse force is used to decrease speed and the friction serves as another braking unit of the system.

It is mentioned here that the parameters EI/ml^4, μ and $\hat{k}$ used in the numerical examples, unless otherwise specified, are set to $(9.4/\pi)^2$, zero and zero, respectively.

For numerical integration of the system (34) the Runge–Kutta method with six-order accuracy is used. Figure 3 shows the trajectories of the moving mass with three different constant velocities vs the location of the mass on the beam. The parameters used in this figure are exactly the same as those used in Ayre *et al.* (1951) and Ting *et al.* (1974). There are three small plots in this figure. The bottom one is related to the case when $\dot{\xi} = 0.25\pi$. The middle and top plots are related to the cases when $\dot{\xi} = 0.5\pi$ and $\dot{\xi} = 0.75\pi$, respectively. The other parameters used in the figure are $\hat{v}_{st} = \hat{M}\hat{g}/48$, $\ddot{\xi} = \hat{f} = 0$ and $\hat{M} = 0.5$. The accuracy of the model then was tested by comparison of Fig. 3 with the results reported by Ayre *et al.* (1951) and Ting *et al.* (1974). It is known that the latter is in agreement with experimental observations.

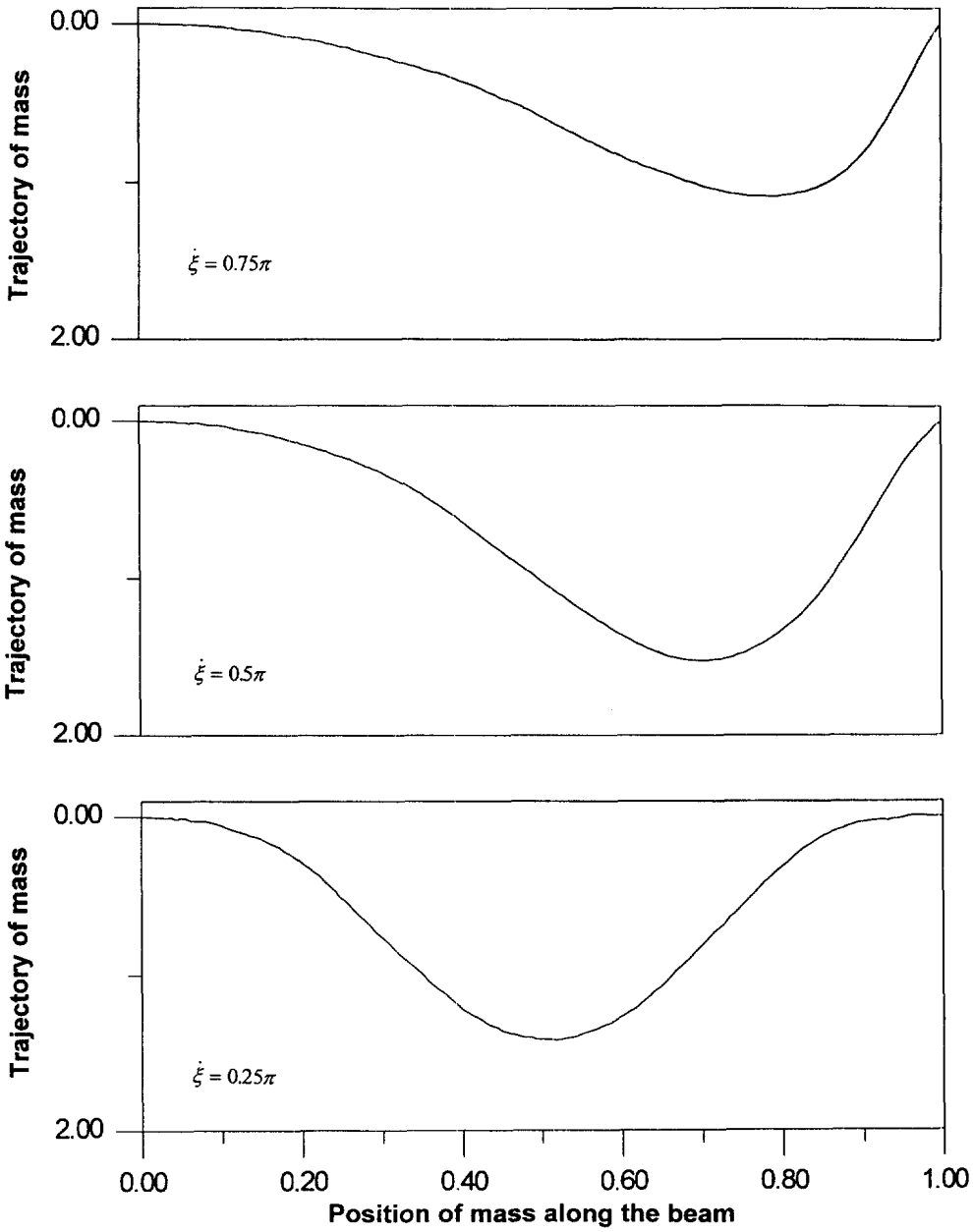

Fig. 3. The trajectory of mass vs the location of the mass along the beam with the same parameters as used in Ayre *et al.* (1951) and Ting *et al.* (1974) for $\dot{\xi} = 0.25\pi$, 0.5π and 0.75π.

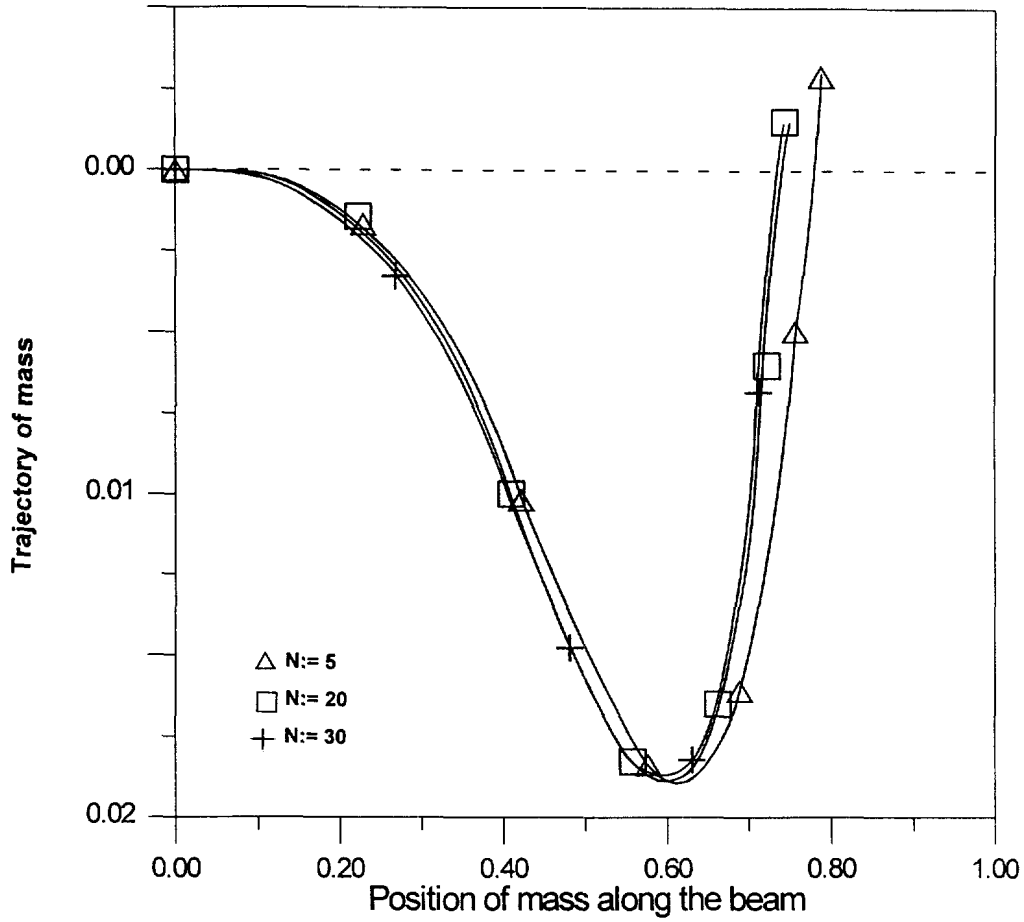

Fig. 4. Rate of convergence of solutions; the trajectory of mass vs the location of the mass along the beam with N for $\dot{\xi}(0) = 0.5\pi$, $\hat{M} = 0.5, \hat{f} = -1.0$ and $\mu = 0.5$.

The dimension N of $\mathbf{z}$ in eqn (34) that was necessary to retain for sufficient accuracy was found to be 30. Figure 4 shows the rate of convergence of the trajectory of mass vs the position of mass along the beam with N for $\dot{\xi}(0) = 0.5\pi$, $\hat{M} = 0.5, \hat{f} = -1.0$ and $\mu = 0.5$. There is negligible difference between the results for $N = 20$ and 30. Hence, all calculations are based on $N = 30$.

As mentioned previously, unlike other papers in which either the velocity or the acceleration of moving mass is assumed to be constant, in this study, the driving force is specified. For example, forward force ($\hat{f} > 0$) increases the speed of mass and reverse force ($\hat{f} < 0$) decreases the speed of mass. The results variable velocity and acceleration and unknown location of the mass along the beam. This is evident in Fig. 5. In the figure, the speed of mass is plotted with the position of mass along the beam with $\hat{M} = 0.5$ for three different values of forward driving force, $\hat{f} = 0.1$, 0.5 and 1.0.

The effect of forward force to the trajectory of mass is illustrated in Fig. 6. This figure shows the trajectory of the mass, $\hat{v}(\xi)$, vs the position of mass along the beam. The parameters used in the figure are the same as those used in Fig. 5. The results indicate that while the mass travels along the beam the deflection of the beam at mass grows with the applied force. Another interesting phenomenon is that when the moving mass is near the end point of the beam, negative displacement occurs if the speed of the mass is not high. This is expected and has been observed by other authors.

In order to investigate the deflection profile of the beam due to the motion of the attached mass at different locations in detail, we chose four different instant positions of the mass on the beam. They are $\xi = 0.2$, 0.5, 0.8 and 1.0. Figures 7 and 8 present the deflection profile of the beam caused by the motion of the attached mass at the four instant locations mentioned above for $\dot{\xi}(0) = 0$ and $\hat{M} = 0.5$. The applied force in the two figures

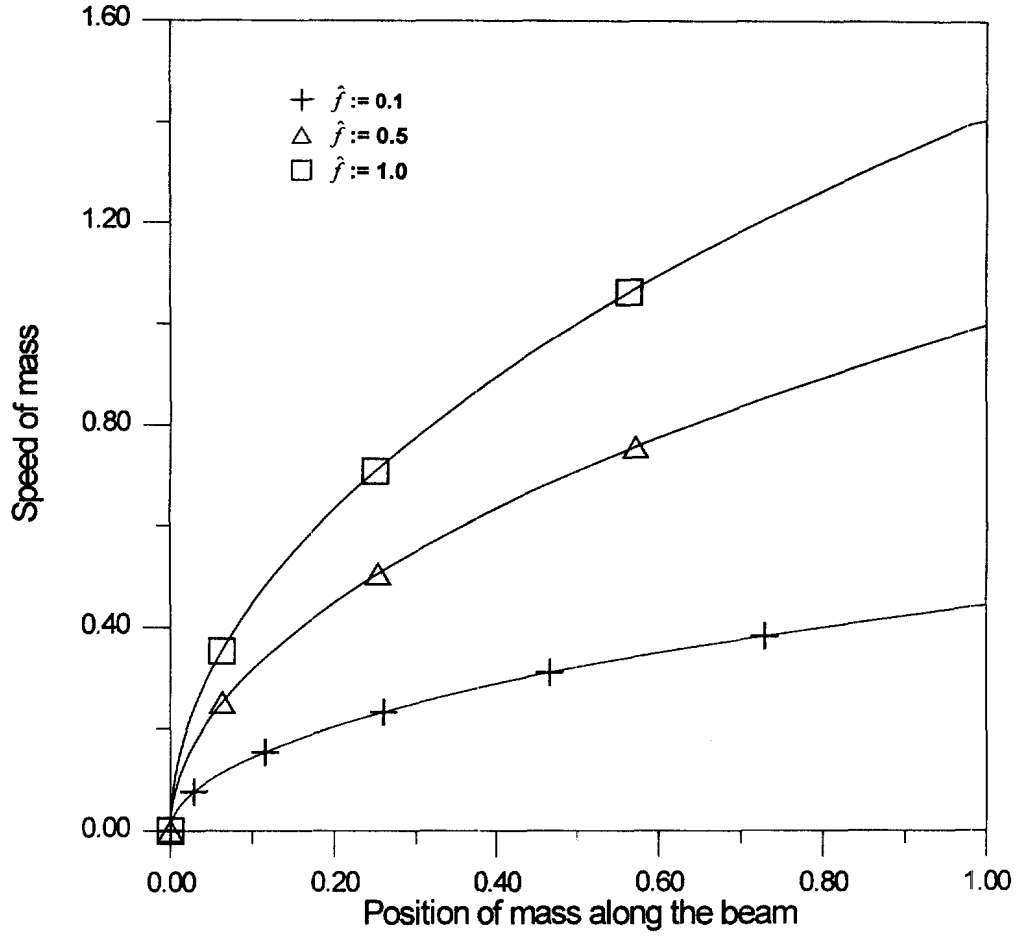

Fig. 5. The speed of mass vs the location of mass along the beam for $\dot{\xi}(0) = 0$, $\mu = \hat{k} = 0$, $\hat{M} = 0.5$ and $\hat{f} = 0.1$, 0.5 and 1.0.

are, respectively, $\hat{f} = 0.1$ and 1.0. Figures 9 and 10 show similar information to that shown in Figs 7 and 8, except in these figures the initial speed $\dot{\xi}(0)$ is set to be 0.25π. The results disclose that the applied force and initial speed of mass have positive effects to the deflection of the beam. They also show that negative displacement vanishes if the driving force is large. In other words, it is generally true that negative displacement does not exist if the speed of mass is high.

As stated before, an important feature to be considered in this study is the ability to bring the mass to a halt at desired position. This can be achieved by applying reverse force to the mass and/or increasing the friction between the mass and the beam. The results are given in Figs 11–13. Figure 11 presents the manner in which the trajectory of the mass develops with the position of the mass along the beam for $\dot{\xi}(0) = 0.25\pi$ and $\hat{M} = 0.5$. The retard forces applied to the mass are $\hat{f} = -0.25$, -0.5 and -0.75, respectively. The results indicate that if a large reverse force is applied to the mass, an acute variation of the displacement of the beam at mass occurs when the moving mass is about to stop. It also shows that in some conditions (for example $\hat{f} = -0.5$), when the mass is going to stop the displacement of beam at mass is upward first and then downward until it stops. This is, perhaps, due to the effects of inertia of the beam and the applied reverse force. Accordingly, the travel speed of mass on the beam is given in Fig. 12.

Figure 13 illustrates similar information to that shown in Fig. 11, except in the figure $\dot{\xi}(0) = 0.5\pi$ and $\hat{f} = -0.5$, -1.0 and -1.5. The results of Figs 11 and 13 show that when the speed of mass approaches zero, negative displacement occurs if large reverse thrust is applied to the mass. However, for the case when the initial speed is slow, this phenomenon, negative displacement, was not found.

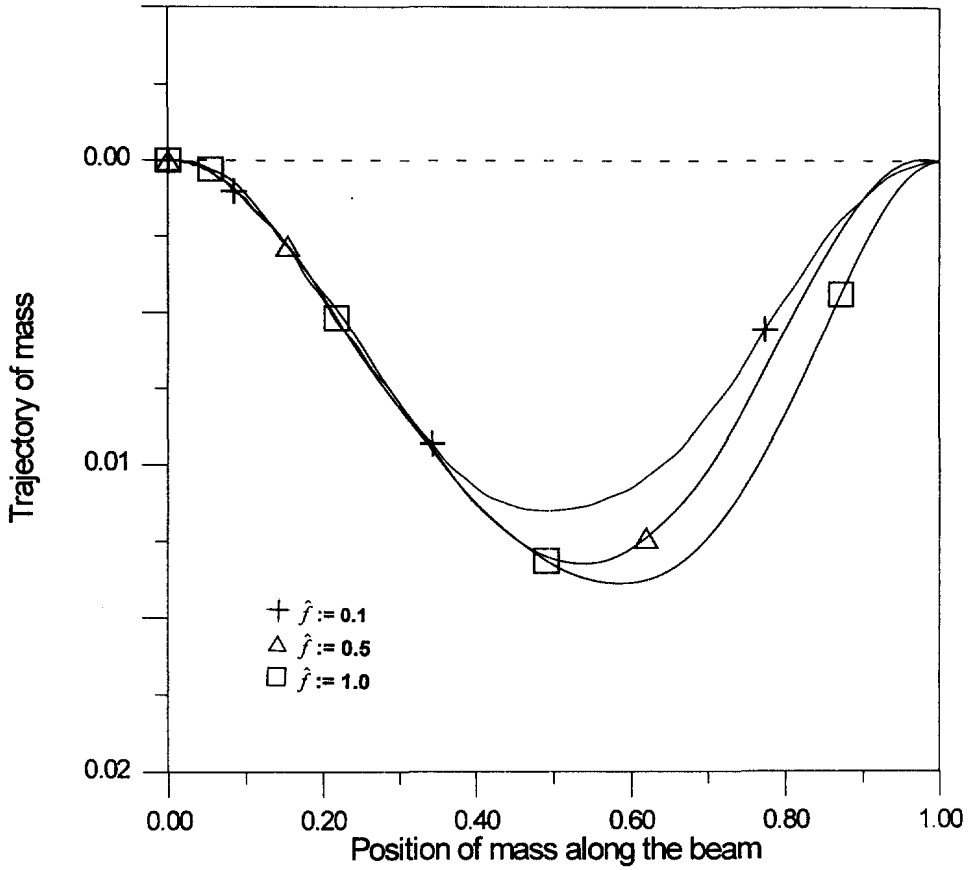

Fig. 6. The trajectory of mass vs the position of mass along the beam with the same parameters as used in Fig. 5.

The effect of friction between the mass and the beam to the motion of the system is given by Fig. 14. This figure shows the trajectory of mass vs the position of mass along the beam for $\dot{\xi}(0) = 0.5\pi, \hat{f} = -1.0$ and $\hat{M} = 0.5$. The coefficient of friction μ in this example is set to be 0.0, 0.25 and 0.5. The result indicates that if the friction is not zero then the retard force required to stop the mass at the desired point decreases as the friction develops.

The influence of the weight of the mass on the motion of the system is given by Figs 15 and 16. Figure 15 presents the effect of the weight of mass to the deflection of the beam at the point where the mass is located on the beam. Three different values of the weight of the mass are chosen: $\hat{M} = 0.5$, 1.0 and 2.0. The other parameters used in this figure are $\dot{\xi}(0) = 0$ and $\hat{f} = 0.5$. Correspondingly, the travel speed of the mass to move along the beam is given by Fig. 16. The results of these two figures disclose that the weight of mass amplifies the displacement of the beam, but has no significant effect on the travel speed.

The effect of elastic foundations to the deflection of the beam, due to the motion of the moving mass, is shown in Figs 17 and 18. In Fig 17, the trajectory of mass is plotted as a function of the position of the mass along the beam for $\dot{\xi}(0) = 0$, $\hat{M} = 2.0$, $\mu = 0, \hat{f} = 0.5$ and $\hat{k} = 0.0$, 100 and 200. As expected, the result shows that increasing of the foundation stiffness reduces the deflection of beam. Meanwhile, negative displacement occurs when the mass is near the end point of the beam. Figure 18 presents the deflection profile of the beam when the mass is located at the end point of the beam, $\xi = 1.0$, with the same parameters as used in Fig. 17. From this figure, we observed that the foundation stiffness seems to have positive effect on the negative deflection of the beam.

CONCLUSIONS

In this study, the dynamics and mechanics of a finite inextensible beam that rests on a uniform elastic foundation and carries an accelerating mass are studied. The moving mass

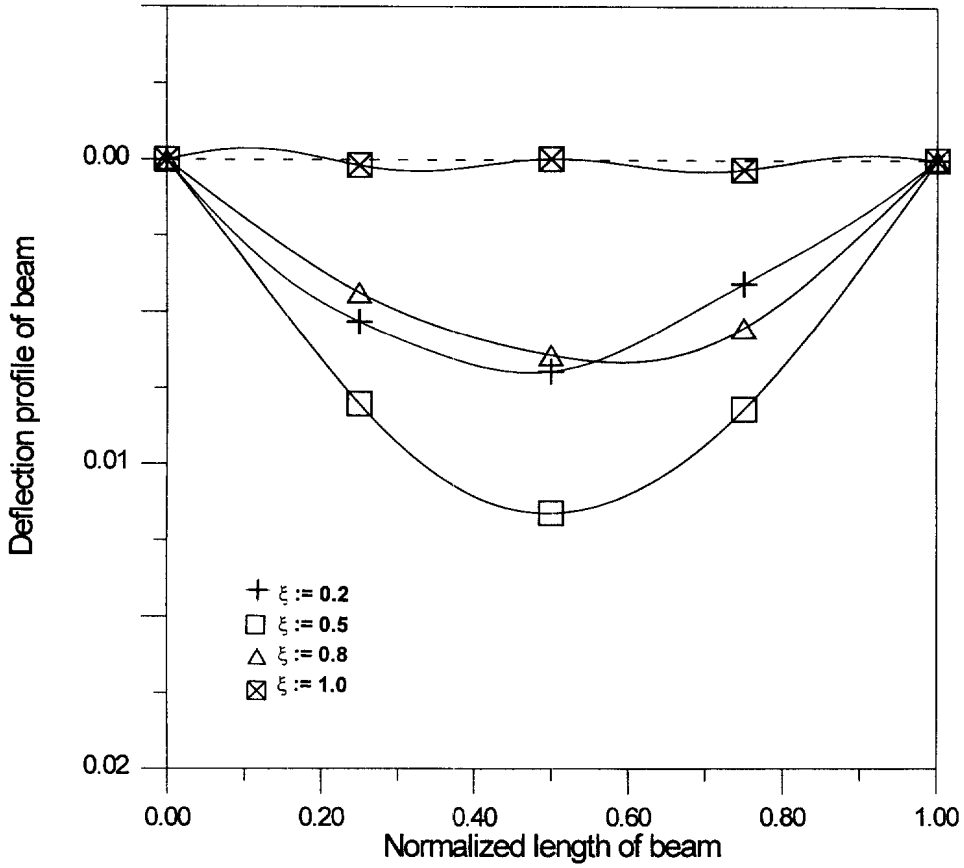

Fig. 7. Deflection profile of the beam due to the motion of the attached mass at four instant positions, $\xi = 0.2$, 0.5, 0.8 and 1.0. The parameters used are $\dot{\xi}(0) = 0$, $\mu = \hat{k} = 0$, $\hat{M} = 0.5$ and $\hat{f} = 0.1$.

is to be accelerated by a forward force and is able to reduce speed and be brought to a halt at a desired position on the beam by a retard force.

The mechanics of the interface between the mass and the beam is determined by modeling the mass as a rigid body that travels on a flexible structure. The interaction force, caused by convective acceleration and friction of the mass moving on the beam, is thus a function of the beam displacement. Therefore, there exists a nonlinear coupling between the deflection of the beam and the function that presents the position of the mass on the beam. The problem of the system is nonlinear.

The numerical integration scheme of the system is obtained by introducing state vectors into the second-order differential equations of motion and, hence, reducing these equations to the first-order state equations with specified initial conditions. The convergence of solutions is achieved when the number of coordinate functions of solutions, denoted as N, is large enough such that the variation of displacements of the beam with N is sufficiently small.

From Figs 5 and 6, we conclude that the applied forward force amplifies the speed of the mass and the displacement of the beam. The ability to bring the mass to a halt at a desired point on the beam is accomplished by applying a constant reverse force to the mass and/or increasing the friction between the mass and the beam after the mass has achieved specified conditions. Figures 11 and 13 show that the applied retard force reduces the speed of the mass. A full stop of the mass occurs if appropriate reverse force is applied to the mass. Moreover, as shown in Fig. 14, if the friction between the mass and the beam is not zero, the reverse force that is required to stop the mass at a desired point decreases as the friction increases. The effect of weight of the moving mass on the system is that the weight

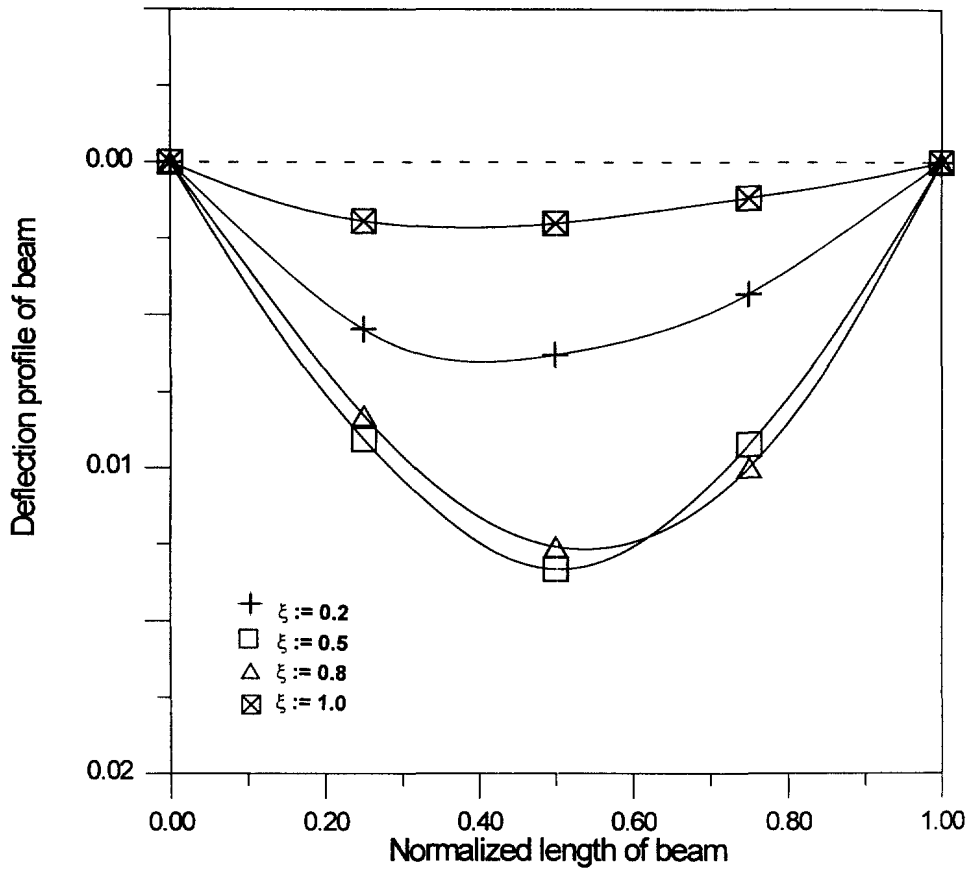

Fig. 8. Deflection profile of the beam due to the motion of the attached mass at four instant positions, $\xi = 0.2$, 0.5, 0.8 and 1.0. The parameters used are $\dot{\xi}(0) = 0$, $\mu = \hat{k} = 0$, $\hat{M} = 0.5$ and $\hat{f} = 1.0$.

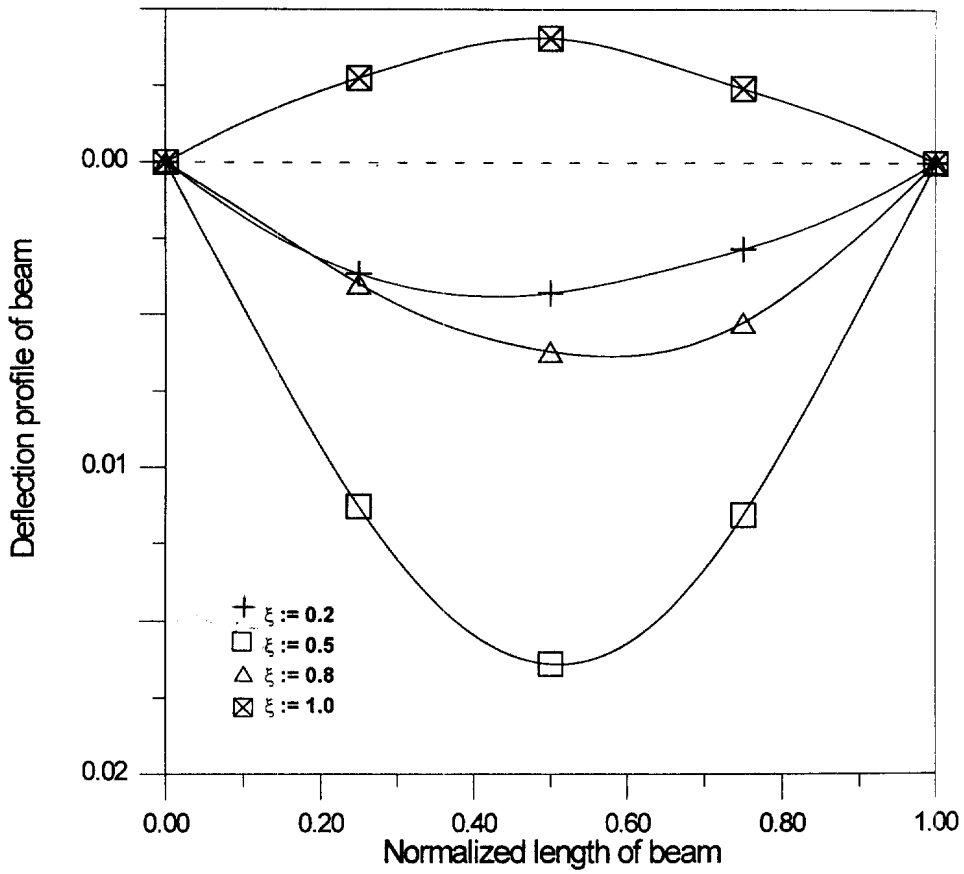

Fig. 9. Deflection profile of the beam due to the motion of the attached mass at four instant positions, $\xi = 0.2, 0.5, 0.8$ and 1.0. The parameters used are $\xi(0) = 0.25\pi$, $\mu = \hat{k} = 0$, $\hat{M} = 0.5$ and $\hat{f} = 0.1$.

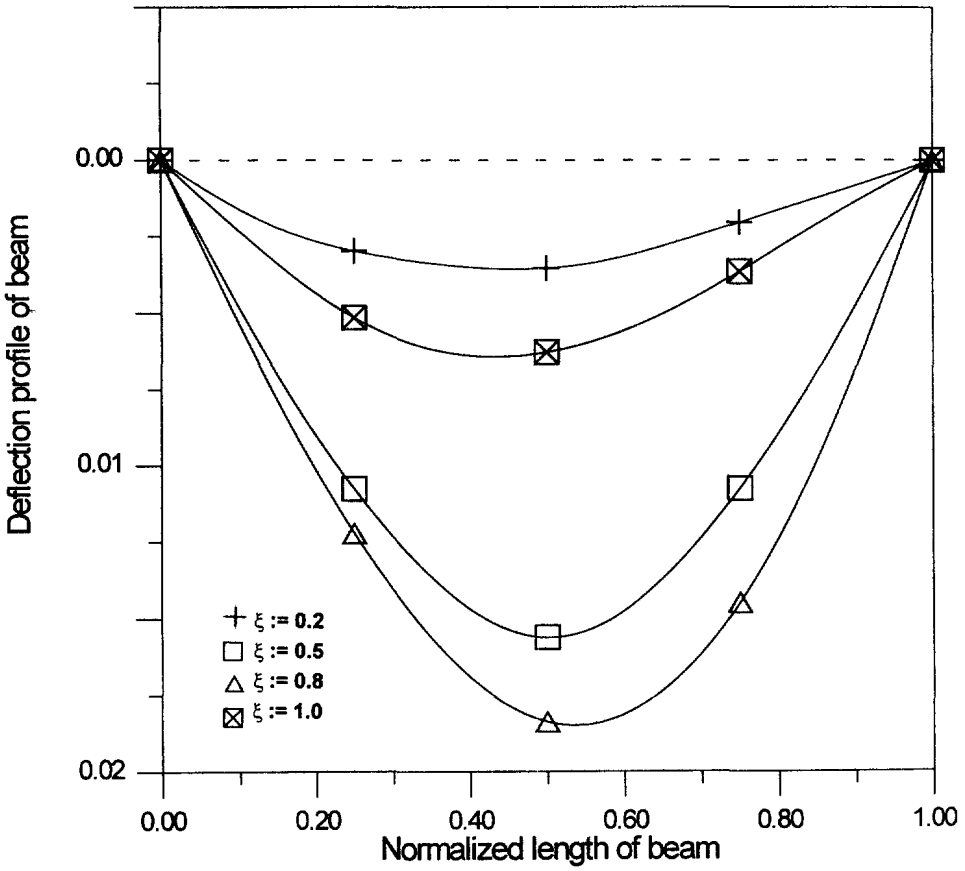

Fig. 10. Deflection profile of the beam due to the motion of the attached mass at four instant positions, $\xi = 0.2, 0.5, 0.8$ and 1.0. The parameters used are $\dot{\xi}(0) = 0.25\pi$, $\mu = \hat{K} = 0$, $\hat{M} = 0.5$ and $\hat{f} = 1.0$.

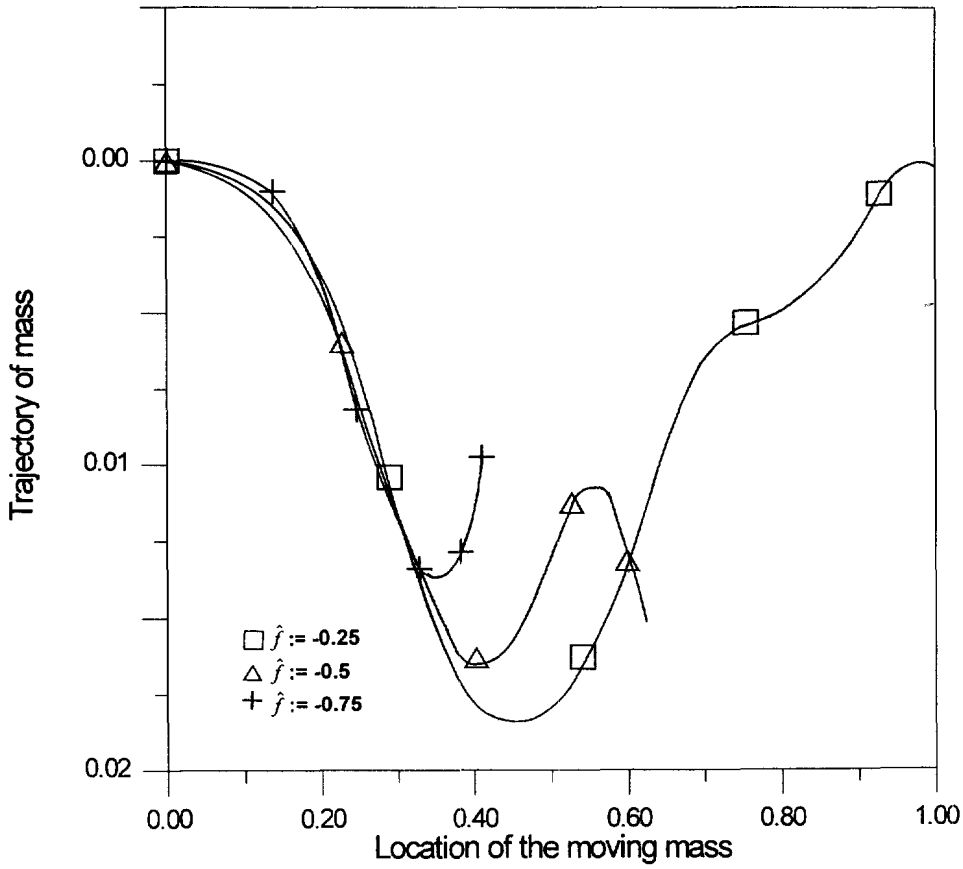

Fig. 11. The variation of the trajectory of mass along the beam. The parameters used are $\dot{\xi}(0) = 0.25\pi$, $\mu = \hat{k} = 0$, $\hat{M} = 0.5$ and $\hat{f} = -0.25$, -0.5 and -0.75.

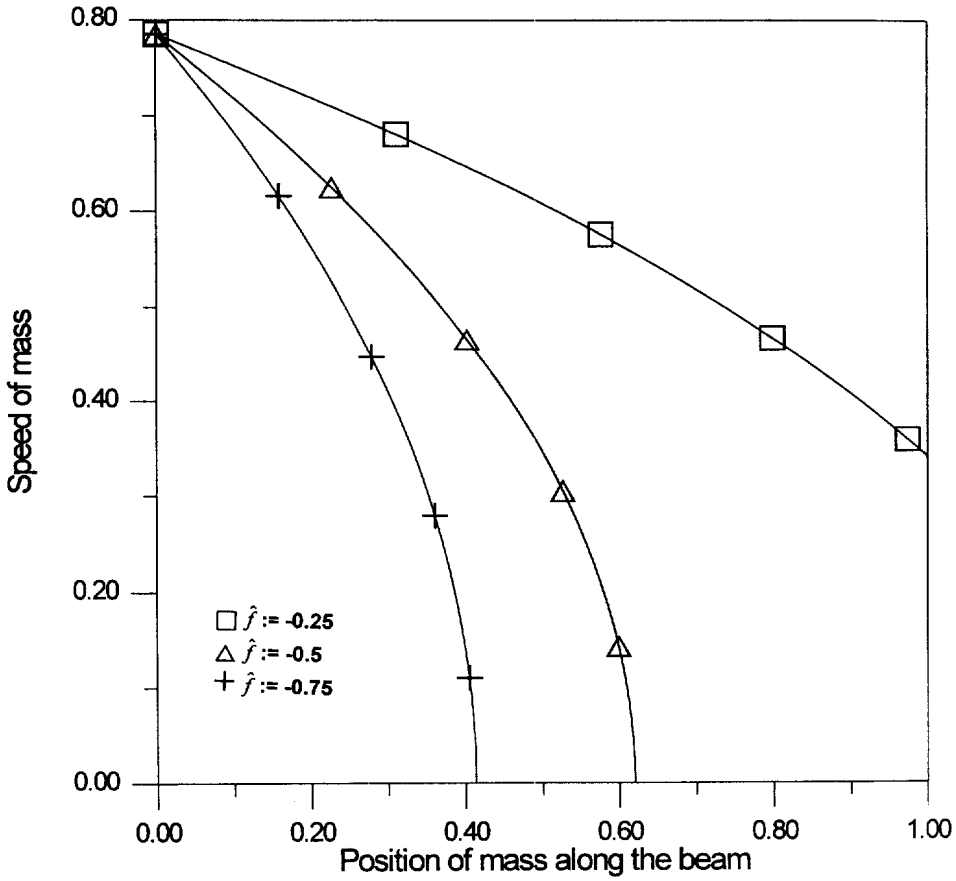

Fig. 12. The variation of travel speed of mass along the beam with the same parameters as used in Fig. 11.

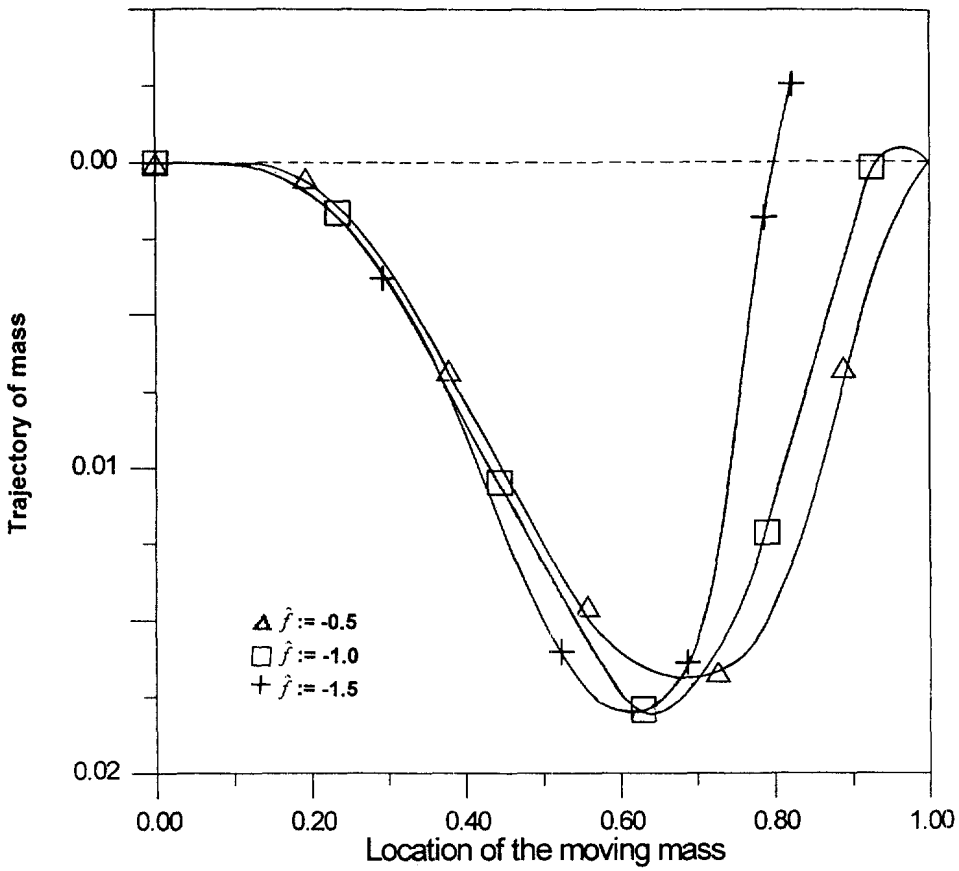

Fig. 13. The variation of the trajectory of mass along the beam. The parameters used are $\dot{\xi}(0) = 0.5\pi$, $\mu = \hat{k} = 0$, $\hat{M} = 0.5$ and $\hat{f} = -0.5$, -1.0 and -1.5.

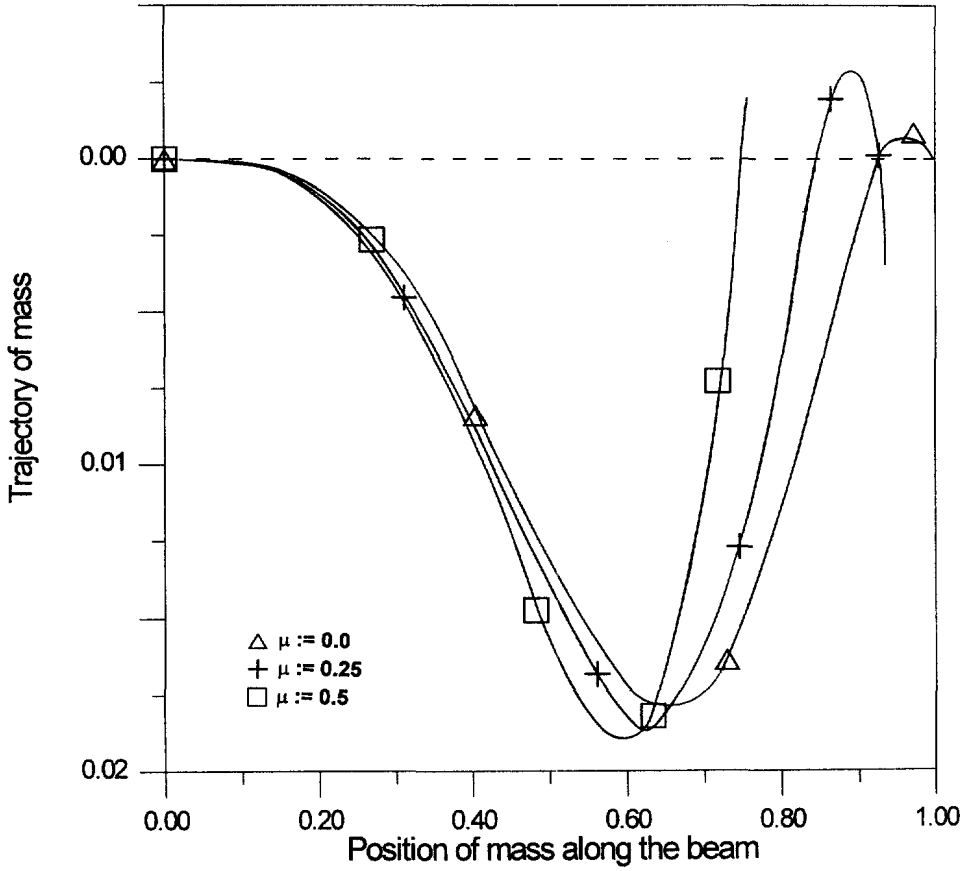

Fig. 14. The variation of the trajectory of mass along the beam. The parameters used are $\dot{\xi}(0) = 0.5\pi$, $\hat{k} = 0$, $\hat{M} = 0.5$, $\hat{f} = -1.0$ and $\mu = 0.0$, 0.25 and 0.5.

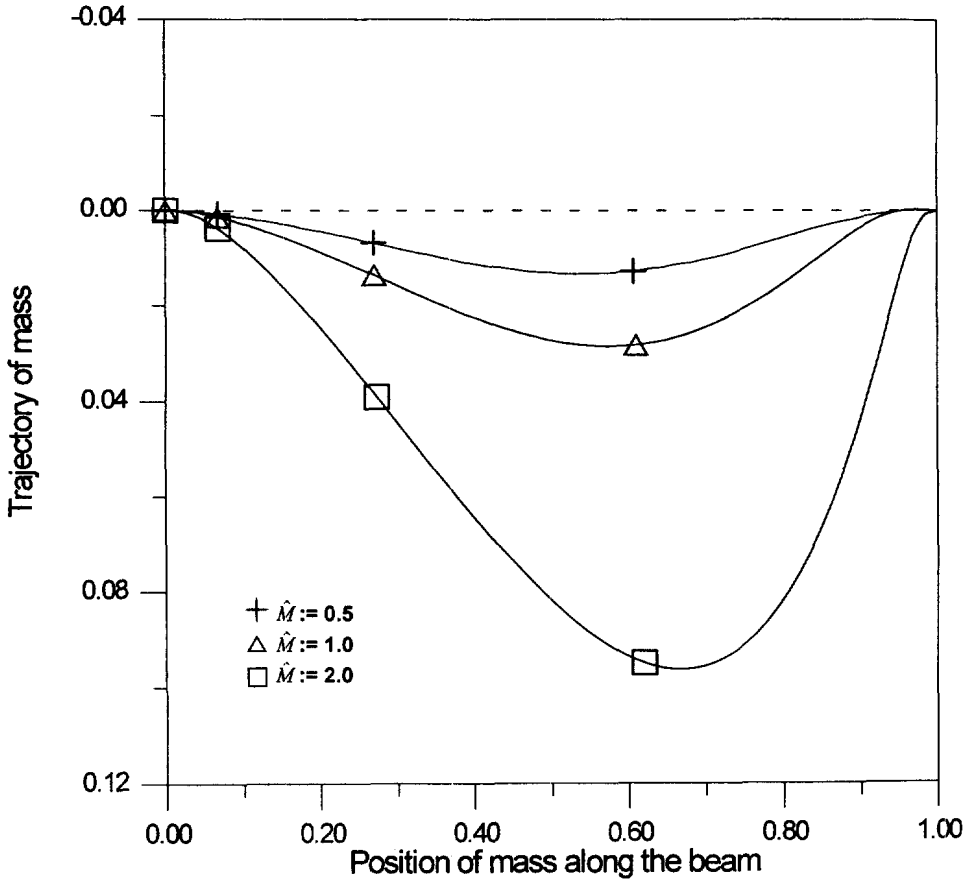

Fig. 15. The variation of the trajectory of mass along the beam. The parameters used are $\dot{\xi}(0) = 0$, $\mu = \hat{k} = 0, \hat{f} = 0.5$ and $\hat{M} = 0.5$, 1.0 and 2.0.

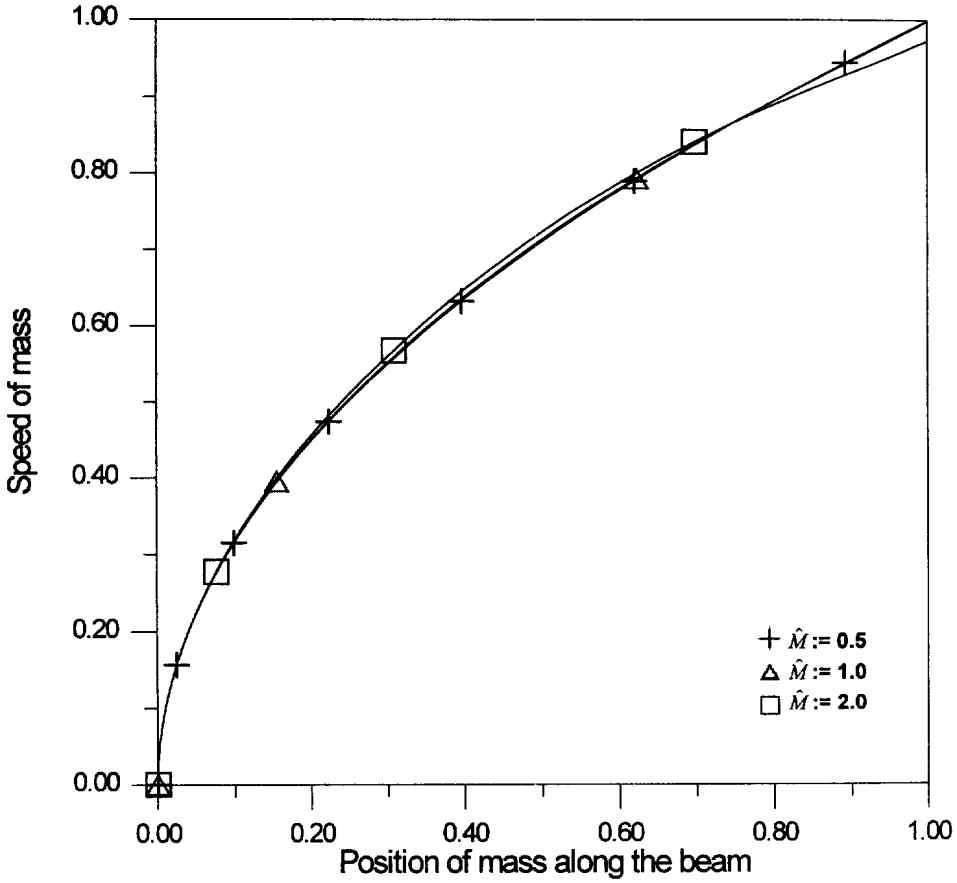

Fig. 16. The variation of travel speed of mass along the beam with the same parameters as used in Fig. 15.

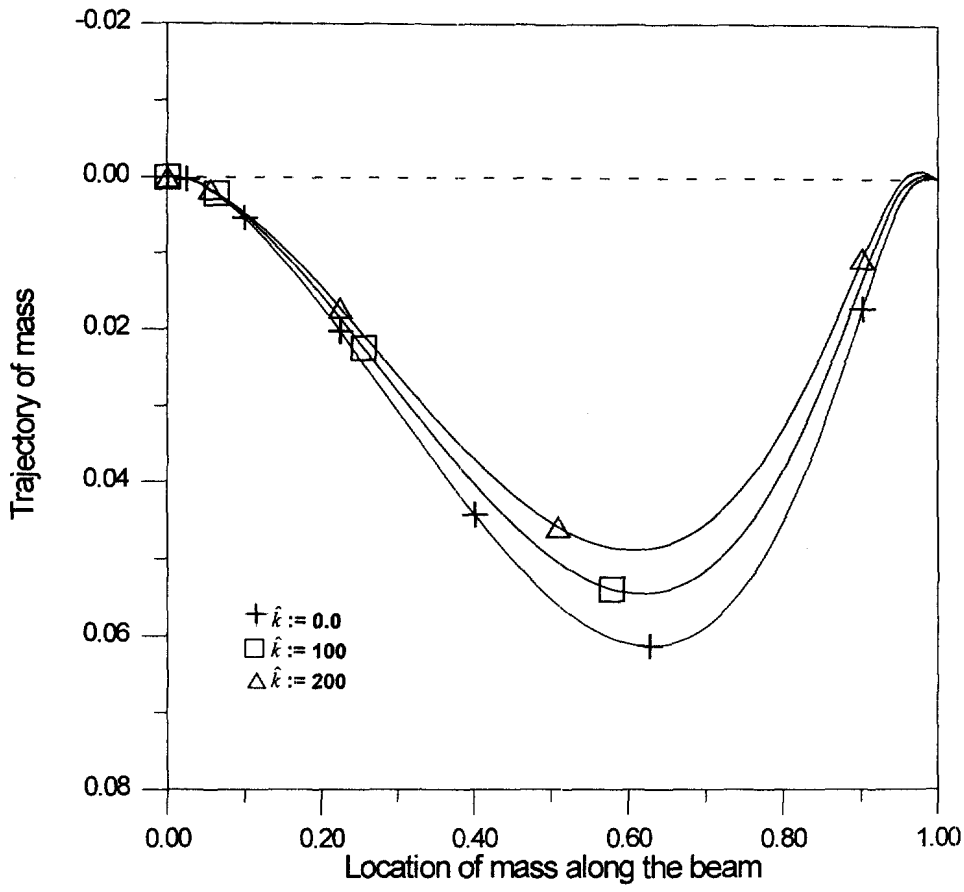

Fig. 17. The variation of trajectory of mass along the beam. The parameters used are $\dot{\xi}(0) = 0$, $\mu = 0, \hat{f} = 0.5$, $\hat{M} = 2.0$ and $\hat{k} = 0.0$, 100 and 200.

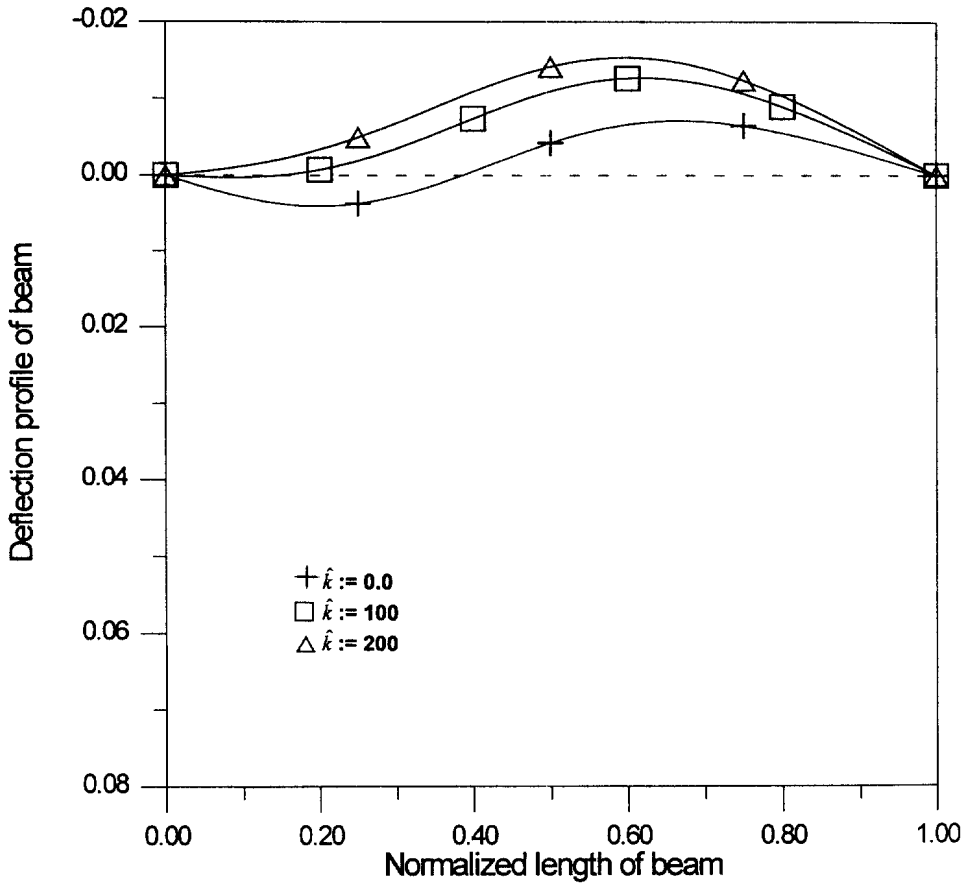

Fig. 18. The deflection profile of the beam when the mass is located at the end point, $\xi = 1.0$. The parameters used are the same as those used in Fig. 17.

of mass amplifies the deflection of the beam, but has no significant result on the speed, as shown in Figs 15 and 16.

Acknowledgements—The work reported here was supported by the National Science Council, Taiwan, under the grant no. NSC85-2212-E-018-005 to National Chunghua Normal University.

REFERENCES

Achenbach, J. D. and Sun, C. T. (1965) Moving load on a flexibly supported Timoshenko Beam. *International Journal of Solids and Structures*, **1**, 353–370.

Alexsandradis, A. A., Dowell, E. H. and Moon, E. C. (1978) The coupled response of a dynamic element riding on a continuously supported beam. *Journal of Applied Mechanics*, **45**, 864–890.

Ayre, R. S., Jacobson, L. S. and Hsu, C. S. (1951) Transverse Vibration of one- and two-span beams under the action of a moving mass loads. *Proceedings of the First National Congress of Applied Mechanics*, pp. 81–90.

Florence, A. L. (1965) Traveling force on a Timoshenko beam. *Journal of Applied Mechanics*, **32**, 351–358.

Fryba, L. (1972) *Vibration of Solids and Structures under Moving Loads*. Noordholt, The Netherlands.

Meirovitch, L. (1967) *Analytical Methods in Vibrations*. Macmillan, New York.

Meirovitch, L. (1970) *Methods of Analytical Dynamics*. McGraw–Hill, New York.

Nelson, H. D. and Conover, R. A. (1971) Dynamic stability of a beam carrying moving masses. *Journal of Applied Mechanics*, **38**, 1003–1006.

Steele, C. R. (1967) The finite beam with a moving load. *Journal of Applied Mechanics*, **34**, 111–118.

Steele, C. R. (1968) The Timoshenko beam with a moving loads. *Journal of Applied Mechanics*, **35**, 481–488.

Steele, C. R. (1971) Beams and shells with moving loads. *International Journal of Solids and Structures*, **7**, 1171–1198.

Tadjbakhsh, I. G. and Wang, Y. M. (1993) The transient vibrations of a taut inclined cable with a riding accelerating mass. *Journal of Nonlinear Dynamics* (submitted).

Ting, E. C., Genin, J. and Ginsberg, J. H. (1974) A general algorithm for moving mass problems. *Journal of Sound and Vibrations*, **33**, 49–58.

Wang, Y. M. (1993) Cable dynamics, Part I: the transient vibrations of a taut inclined cable with a riding accelerating mass. Ph.D. thesis, Rensselaer Polytechnic Institute, Troy, New York.

APPENDIX

$\mathbf{M} = [M_{jn}]$, $M_{jn} = \delta_{jn} + 2\hat{M}\hat{S}_{jn}$

$\mathbf{N} = [N_{jn}]$, $N_{jn} = 4\hat{M}R_{jn}$

$\mathbf{K}_1 = [K_{1jn}]$, $K_{1jn} = ((j\pi)^4 + \hat{k})\delta_{jn} - 2\hat{M}\hat{f}R_{jn}$

$\mathbf{K}_2 = [K_{2jn}]$, $K_{2jn} = 2\hat{M}R_{jn}$

$\mathbf{K}_3 = [K_{3jn}]$, $K_{3jn} = -2\hat{M}S_{jn}$

$\mathbf{h} = (h_j)$, $h_j = 2\hat{M}\hat{g}\hat{S}_j$

$\mathbf{s} = (S_n)$

$\mathbf{c} = (C_n)$

$p(\xi, \mathbf{y}) = \mu \mathbf{s}^{\mathrm{T}}\mathbf{y}$, $\mathbf{s} = (S_n)$

$q(\xi, \mathbf{y}) = -2\mu \mathbf{c}^{\mathrm{T}}\dot{\mathbf{y}}$, $\mathbf{c} = (C_n)$

$f^* = \hat{f} - \mu\hat{g}$

$\tilde{\mathbf{c}}(\xi) = -\hat{g}\mathbf{c}$

$\tilde{\mathbf{s}}(\xi) = -\mu\mathbf{s}$.